

# THE DIFFRACTION LIMITED APERTURE OF THE ATMOSPHERE AND ITS EFFECTS ON FREE SPACE LASER COMMUNICATIONS

by

Gary D. Wilkins  
Avionics Directorate  
Wright Laboratory

This paper summarizes the Wright Laboratory In-House Laboratory Independent Research (ILIR) conducted to determine the feasibility of using inherent information, such as angle-of-arrival fluctuations of incident radiation and spreading of the focused spot size, obtained through the measurement of the diffraction limited aperture of the atmosphere ( $r_0$ ), to adaptively optimize laser communications system parameters. The method used to measure the  $r_0$  and details concerning the 8 kilometer pulsed laser communications link established between the Wright Patterson AFB Trebein Test Site and Area B Building 620 Laser Communications Laboratory (LCL) are described.

Upon arriving for work in Wright Laboratory's Laser Communications Laboratory (LCL) one morning just before daybreak in early November 1991, I cast my eyes over the city of Dayton and saw a googol of lights twinkling in the darkness. Then I wondered what the diffraction limited aperture of the atmosphere (DLAA) was that morning. I went over to the MicroVAX computer which had been collecting  $r_0$  data from the night before and found that the DLAA was 1.5 centimeters. I then checked my Bit Error Rate Tester (BERT) on the laser communications data link and found it not even registering. Then I looked at the signal on the oscilloscope and watched it pop in and out of the noise with amplitude variations exceeding 30db.

One of the most important items to consider when using free space laser communications in an atmospheric environment is the atmosphere. Whether communication is from air-to-air or air-to-ground, the atmosphere plays a major role in corrupting it. Moisture, aerosols, temperature and pressure changes produce refractive index variations in the air by causing random variations in

density. These variations are referred to as eddies and have a lens effect on light passing through them. When a plane wave passes through these eddies, parts of it are refracted randomly causing a distorted wavefront with the combined effects of variation of intensity across the wavefront and warping of the isophase surface [3]. By the time the light reaches its destination, it is no longer spatially or temporally coherent over the entire wavefront and an optical system sampling a large portion of the wavefront would not be able to focus the light to the diffraction limit of the optics. Instead, the size of the airy disk produced would be a function of the diffraction limited aperture of the atmosphere, or transverse phase coherence length,  $r_0$ , as it is commonly called. An optical system which has an aperture equal to or less than the  $r_0$  will sample a coherent portion of the wave and produce an image that is based upon the quality of the optical equipment. If the aperture of the optical equipment is larger than the  $r_0$ , then the quality of the image will be dependent upon the amount of atmospheric turbulence in the optical path. The following diffraction equation shows the relationship of the telescope aperture,  $D$ , the wavelength of light,  $\lambda$ , and the focal length of the optical system,  $f.l.$ , to the size of the focused spot, airy disk diameter, in a turbulent free environment:

$$\text{AiryDiskDiameter} = 2.44(\lambda * f.l.) / D \quad 1-1$$

Knowing that using an optical system with an aperture greater than the  $r_0$  will produce a focused spot size which is dependent upon the diffraction limited aperture of the atmosphere allows us to

replace the telescope aperture,  $D$ , in the diffraction equation with  $r_0$ . The following equation is the relationship between the Airy Disk Diameter and the effective aperture,  $r_0$ , which caused the increase in the size of the airy disk:

$$r_0 = \frac{2.44(\lambda * f.l.)}{(AiryDiskDiameter)} \quad 1-2$$

The size of the resultant airy disk formed at the focus of the optical system determines the amount of energy which will be available to a detector of finite size, and the atmospheric turbulence induced beam wander determines the location of the spot on (or off) the detector. Because of this, we set out to develop a system to monitor the  $r_0$  to determine the stochastic nature of the communications medium. We are then able to investigate the feasibility of using the  $r_0$  information to adapt laser communications system parameters (i.e. data rate, transmit power, etc.) for the purpose of optimizing the communications process in the presence of atmospheric turbulence. To accomplish this goal, two things were needed; (1) a long distance free space laser communications link with the capability of measuring the bit error rate, and (2) a system to measure the characteristics of the atmosphere in near real time.

To accomplish this research, an 8 kilometer pulsed laser communications link has been established between the WPAFB Trebein Test Site and the Laser Communications Lab (LCL) located on the twelfth floor of the Area B Building 620 tower. A block diagram of the laser communications link is shown in Figure 1.

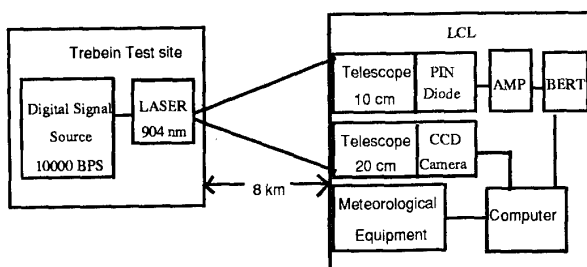


Figure 1. Laser Communications link

The laser transmitter and bit error rate encoder are located at the Trebein Test Site and the re-

ceiver,  $r_0$ , meteorological, and data acquisition equipment are in the LCL. The laser transmitter is a Laser Diode, Inc. LT-201 capable of 100 watts peak optical output power, but is currently being operated at 20 watts peak. It operates at a wavelength of 904 nanometers and a beam divergence of 1 milliradian. The transmitter is edge triggered by the return to zero TTL output of a bit error rate encoder operating at a clock frequency of 10 KHz, and emits a 40 nanosecond pulse for each positive transition of the data input signal.

The laser receiver was designed and built in-house. It consists of a Celestron 90mm Maksutov Cassegrain spotter scope adapted to focus light onto a silicon photodiode housed with a 10 nm bandpass filter in a Melles Griot modular photodetection system. A Melles Griot 13AMP005 Wide Bandwidth Detector Amplifier supplies current to the detector and acts as the first stage amplifier. The signal is then amplified by a Stanford Research Systems Model SR560 low noise amplifier which supplies the needed gain and electronic filtering. The resulting 40 microsecond Gaussian shaped pulses are converted into TTL level square pulses with a function generator and subsequently fed into an HP 3780A Bit Error Rate Tester (BERT) for analysis.

Another device which had to be developed and built in-house was the device for measuring  $r_0$ . We decided to draw upon past experience and design a system which could be useful for our work in laser communications. One of the earliest methods of determining  $r_0$  involved photography. Light from a distant star was focused onto a photographic plate, and after a suitable exposure time the plate was developed. The diameter of the focused spot was then determined with the aid of a densitometer and a mechanical measuring device, and the  $r_0$  calculated. Even though one could conceivably use an automatic camera to take a sequence of pictures over a period of time, this was a rather slow process. As interest in the stochastic nature of the atmosphere grew and technology advanced, other methods of measuring the seeing condition of the atmosphere were developed.

A past endeavor of mine involved developing a method of measuring the  $r_0$  for use as a tool to

help characterize the atmosphere for surveillance applications. A one meter aperture cassegrain telescope was used to gather incoming light from a point source and focus it onto a spinning reticle wheel which contained a track of apertures which increased geometrically in size [16]. Light passing through the apertures of the reticle was collected by a photomultiplier, and the resulting electrical signal was digitized by an analog-to-digital converter. The digital output contained information about the modulation transfer function of the atmosphere, and this was reduced by a computer to provide the diffraction limited aperture of the atmosphere. The system was large, even without the 1 meter telescope, and the optics were difficult to keep aligned due to atmospheric boundary layer induced beam wander. Although the system was good for its time, its size and mechanical parts were impractical for use as a real time atmospheric turbulence monitor for laser communications systems.

A third method of obtaining the  $r_0$  is to measure the refractive index structure parameter,  $C_n^2$ , using a stellar scintillometer. This method involves taking several scintillation measurements along the optical path and deriving the  $C_n^2$  information analytically. The  $r_0$  can then be derived by using an equation which relates  $r_0$  to  $C_n^2$ . Although this method does arrive at the  $r_0$ , we felt that a system which measured  $r_0$  directly would better serve our laser communications work. Since the condition of the atmosphere is constantly changing because of the wind, temperature, and pressure changes; so is the refractive index and the DLAA. Therefore, a direct measurement of the  $r_0$  is required to provide information fast enough to make the required communications parameter changes to achieve an optimum communications channel.

The  $r_0$  measuring system built for this research incorporates the simplicity of the photographic method with the data acquisition capability of the rotating reticle wheel method, without the need for chemicals or mechanical devices. The device consists of a Celestron Classic 8 f/10, 20.3 cm aperture Schmidt-Cassegrain telescope which focuses the light from the laser onto a VIDEK camera CCD array. The array has an active image area

containing 1320 (horizontal) by 1035 (vertical) pixels positioned back to back to obtain a unity fill-ratio that is 8.98 mm in the horizontal and 7.04 mm in the vertical. A built-in 8 bit A/D converter produces a digital video output signal containing 256 gray levels. The digitized image of the fourier transform of the incoming plane wave is then processed by a Univision UDC-500Q frame grabber residing in a Q bus slot inside a MicroVAX computer, and is displayed on a high resolution Sampo monitor connected directly to the UDC-500Q video output connector.

Computer code required by the frame grabber to control the camera output, process the image data, and display the image was supplied by Univision as part of the UDC-500Q demonstration package. However, since the supplied programs only allowed the camera to be operated in a continuous mode of approximately 1 frame per second with no ability to control the length of exposure or rate at which the device took the exposures, it was decided to write new software from scratch. After considerable experimentation was conducted by turning on different bits in the UDC-500Q address and monitoring which control lines were affected, software was written to trigger the camera on queue and to vary the exposure time from the minimal allowable exposure of the camera, 14 milliseconds, to as long as the operator desires. The ability to detect the edges of the airy disk, determine its diameter, calculate the  $r_0$ , and archive the results to the hard disk were also incorporated into the code. The process takes approximately 8.5 to 10 seconds per measurement depending upon the exposure length required to obtain the sample.

The whole system was built in stages in the laboratory. The transmitter first, and the  $r_0$  measuring system next. The receiver evolved from a simple detector connected to an oscilloscope, to the system described earlier. Since the  $r_0$  measuring system and the transmitter were finished first, much more  $r_0$  data has been collected than BER data. The  $r_0$  was collected at 8 to 10 second intervals from the beginning of January 1991 until the end of June 1991. It consists of measurements as small as .5 cm to as large as 20 cm using exposure lengths of 10 milliseconds to as great as 2000 mil-

liseconds. BER data was a little more difficult to collect since the communications link had to be synchronous because of the BERT. Scintillation induced signal amplitude variations exceeding 20 dB caused timing variations (jitter), between the received signal and BERT clock, as great as 30 microseconds. This, in turn, would cause the BERT to go out of sync and dump the data collected over its one minute forty second update cycle. Because of the long update cycle, approximately eight  $r_0$  samples were collected for each BER sample obtained with minimum jitter. With a great deal of jitter or decreased visibility, the communications system would not produce a BER sample. The net result is that, to date, we have obtained much more data concerning the stochastic nature of the communications channel than we have actual quantitative data concerning how communications reacts in the channel.

The data we did obtain contains some very interesting observations which should be taken into consideration by laser communications developers. Most of the time, the data collected behaved as one might think it should. An increase in  $r_0$  would cause an improvement in the quality of the received signal, and there would be a corresponding low BER. However, there were also cases contrary to this. On several occasions the BER actually went up (signal quality went down) with increasing  $r_0$ . Knowing that the equipment was functioning properly, there is only one logical explanation for this behavior. An optimum signal is achieved when the size of the airy disk is equal to or less than the active area of the detector as depicted in Figure 2a. A decrease in  $r_0$  will cause an increase in the size of the airy disk and eventually some of the energy contained in the received signal is focused outside the active region of the detector as in Figure 2b. This causes a corresponding increase in the BER as would be expected. Figures 2c and 2d help explain the case for decreasing BER with decreasing  $r_0$ . If the airy disk is located off the active area of the detector near the edge, as in Figure 2c, during a period of large  $r_0$ , there will either be no signal or a very large BER because only some of the energy is being detected. As the size of the airy disk increases due to decreasing  $r_0$ , part of the en-

ergy is seen by the detector as in figure 2d and a corresponding drop in BER takes place.

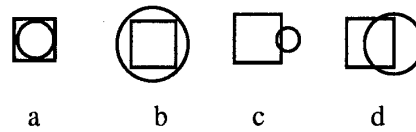


Figure 2. Positioning of a round airy disk on a square detector.

The reasons for the airy disk being located outside the active detector region, as in Figure 2c, can be twofold. First, it may be a simple act of misalignment. The second reason involves the atmosphere and its ability to induce angle-of-arrival changes on the incident radiation. The communications link used for this project is a near horizontal path with a mean height above ground of approximately 120 feet. The path is over a city called Beavercreek, two shopping malls and associated parking lots, an interstate highway, a residential area, a forest, and a marsh area. During the course of the day, each part of the path contributes to the diurnal temperature variations differently. The result is that the incident radiation is bent a little for each refractive index change caused by a temperature/humidity variation. The net result shows up at the receiver as a deviation in the angle-of-arrival and determines the location of the airy disk on (or off) the detector. We know this is happening because we designed our  $r_0$  measurement system to measure the diameter of the airy disk, and to keep track of where the disk is located on the CCD array. Thus we have the ability to determine the angle-of-arrival of the incident radiation. Because of this, we have measured variations in angle of arrival as great as .15 degrees over a four hour period. This corresponds to a dislocation along the focal plane of approximately 250 pixels or 1.7 millimeters, over that period. This may not seem like much until you consider that the field-of-view of the telescope used to measure the  $r_0$  is only .6 degrees, and the detector used for the communications receiver only has an active area diameter of 2 mm. What can happen is that if the alignment

was initially set so that the airy disk was in the center of the detector, it wouldn't be long before the energy of the incident radiation was escaping detection.

At this point, one might ask "Why not use a detector which has an active area large enough to work under all sizes of  $r_0$  and the full field-of-view of the optical system used to capture the incident radiation?" The answer is that as the area of the photodiode increases, so does the junction capacitance and the rise and fall times (diode speed decreases) and it becomes more susceptible to background noise. We initially used a photodiode with a 17mm diameter active region and the signal jitter was so great that the BERT would not sync to the signal except under non turbulent conditions.

We have attempted during this program to ascertain how free space laser communications using direct photodetection is affected by the presence of atmospheric turbulence, and the consequences of a small  $r_0$  and boundary layers in the atmosphere. By doing this, we hope to be able to gather enough insight into the problems of direct photodetection free space laser communications to develop an automated system which can adapt itself to obtain an optimum link in the presence of atmospheric turbulence. The data collected thus far clearly shows that there are forces at work in the atmosphere which cannot be ignored. From this it is obvious that a good laser communications system design depends not only on the diffraction limit of the optics used to focus the signal onto the detector, but also takes into account the diffraction limit of the environment in which it is intended to be used.

The algorithm which has been developed to measure the diffraction limited aperture of the atmosphere can be expanded to control the communications process. With suitable interfaces, the computer can control the amount of gain supplied by the amplifier, the transmit power and beam divergence, data rate, and encoding. It could, if the system designer so desired, even be used to control the size of the aperture on variable aperture systems. Since it is more than likely that a CCD or CID array will be used in the acquisition and tracking process anyway, there is no reason why

the acquisition and tracking algorithm couldn't be part of the algorithm that measures the  $r_0$ , sharing the same computer resources. The result will be a computer based system which will monitor atmospheric turbulence and tracking, and make adjustments as necessary to insure optimum communications through a turbulent atmospheric environment.

## Bibliography

1. Andrews, Harry C., Tutorial and Selected Papers in Digital Image Processing, (various authors), IEEE Inc., New York, NY 1978.
2. Dereniak, Eustace L. and Crowe, Devon G., Optical Radiation Detectors, New York, John Wiley and Sons, 1984.
3. Fried, D.L. 1966, "Limiting Resolution Down Through the Atmosphere", J Opt Soc AM Vol. 56 No 10
4. Fried, D.L. 1966, "Optical Resolution Through a Randomly Inhomogeneous Medium for Very Long and Very Short Exposures", J. Opt Soc. AM., Vol. 56, No. 1372
5. Fried, D.L., 1967, "Optical Heterodyne Detection of an Atmospherically Distorted Signal Wavefront" Proceedings of the IEEE, vol. 55 No.
6. Fried, D.L., 1967, "Atmospheric Modulation Noise in an Optical Heterodyne Receiver", IEEE Journal of Quantum Electronics, Vol. QE-3, No.
7. Fried D.L. and Mevers, G.E. 1974, "Evaluation of  $r_0$  for propagation down through the atmosphere", Applied Optics, Vol. 13, No. 112620
8. Gagliardi, Robert M. and Karp, Sherman, Optical Communications, New York, John Wiley and Sons, 1976.
9. Goodman, Joseph W., Introduction to Fourier Optics, New York, McGraw-Hill Book Co., 1968.
10. Goodman, Joseph W., Statistical Optics, New York, John Wiley and Sons, 1985.
11. Green, William B., Digital Image Processing: A Systems Approach, New York, Van Nostrand Reinhold, 1989.
12. Hall, Ernest L., Computer Image Processing and Recognition, New York, Academic Press, Inc., 1979.

13. Kyle, Thomas G., Atmospheric Transmission Emission and Scattering, New York, Pergamon Press, 1991

14. Rytov, Sergei M., Kravtsov, Yurii A., and Tatarskii, Valeryan I., Principles of Statistical Radiophysics, Berlin Germany, Springer-Verlag, 1987

15. Tatarskii, V.I., Wave Propagation in a Turbulent Medium, McGraw Hill, 1961

16. Wilkins, Gary D., "Measurement of the Atmospheric Phase Coherence Length,  $r_0$ ," In-house report RADC-TR-86-192, December 1986.

17. Yaroslavsky, L. P., Digital Image Processing, New York, Springer-Verlag, 1985.